frontiers in Earth Science

ORIGINAL RESEARCH
published: 13 December 2021
doi: 10.3389/feart.2021.779578

Deterioration and Cavity of Surrounding Rocks at the Bottom of Tunnel Under the Combined Action of Heavy-Haul Load and Groundwater: An Experimental Study

Zheng Li[1,2,3], *Kunping Chen*[4]*, *Ziqiang Li*[5,6], *Weiwei Huang*[5] *and Xinsheng Wang*[4]

[1]School of Civil Engineering, Chongqing University, Chongqing, China, [2]Chongqing University Industrial Technology Research Institute, Chongqing, China, [3]Chongqing City Construction Investment (Group) Co., Ltd., Chongqing, China, [4]School of Resources and Safety Engineering, Chongqing University, Chongqing, China, [5]School of Civil Engineering and Architecture, Chongqing University of Science and Technology, Chongqing, China, [6]Key Laboratory of New Technology for Construction of Cities in Mountain Area, Ministry of Education, Chongqing University, Chongqing, China

OPEN ACCESS

Edited by:
Jie Chen,
Chongqing University, China

Reviewed by:
Wang Tongtao,
Chinese Academy of Sciences (CAS), China
Shi Xilin,
Institute of Rock and Soil Mechanics (CAS), China
Junbao Wang,
Xi'an University of Architecture and Technology, China

***Correspondence:**
Kunping Chen
chen.kp@qq.com

Specialty section:
This article was submitted to Geohazards and Georisks, a section of the journal Frontiers in Earth Science

Received: 19 September 2021
Accepted: 15 November 2021
Published: 13 December 2021

Citation:
Li Z, Chen K, Li Z, Huang W and Wang X (2021) Deterioration and Cavity of Surrounding Rocks at the Bottom of Tunnel Under the Combined Action of Heavy-Haul Load and Groundwater: An Experimental Study. Front. Earth Sci. 9:779578. doi: 10.3389/feart.2021.779578

In China, the first tunnel was built in accordance with the 30-ton heavy-haul railway standard. Based on the change in water and soil pressure obtained from long-term on-site monitoring, the cavity mechanism of the surrounding rock at the bottom of a heavy-haul railway tunnel under rich water conditions was explored in this study. The cavity characteristics and degradation depth of the three types of surrounding rock under different axial loads and hydrodynamic pressures were analyzed through laboratory tests. The structural defects at the bottom of the tunnel and local cracks in the surrounding rock were determined to provide a flow channel for groundwater. The dynamic load of heavy-haul trains causes groundwater to exert high hydrodynamic pressure on the fine cracks. The continuous erosion of the bottom surrounding rock leads to a gradual loss of surrounding rock particles, which would further exacerbate with time. The cohesive soil surrounding rock is noticeably affected by the combined action of heavy-haul load and groundwater in the three types of surrounding rock, and the surrounding rock cavity is characterized by overall hanging. In the simulation experiment, the particle loss of the surrounding rock reached 1,445 g, which is 24.2% higher than that of the pebble soil surrounding rock and 40.8% higher than that of sandy soil surrounding rock. The findings of this study could be helpful for developing methods for defect prediction and treatment of heavy-haul railway tunnels.

Keywords: heavy-haul railway tunnel, field test, train load-groundwater, laboratory test, tunnel bottom cavity

INTRODUCTION

At present, heavy-haul railway transportation has become one of the major means of transportation of global trade goods. Owing to their large volume, low cost, and high efficiency, heavy-haul railways have been widely promoted and used worldwide. In addition, the characteristics of heavy-haul railways, such as large axle loads, large total weights, high traffic densities, and large traffic volumes, have a significant dynamic impact on the structure of the bottom of a tunnel, greatly reducing the

operation state and service life of the tunnel structure. When the heavy-haul railway tunnel is built within a surrounding rock environment with groundwater development, the damage to the structure of the tunnel bottom is more severe under high frequency and large axle loads (Hong, 2000; Zou et al., 2016; Wu et al., 2017). Through the investigation of diseases of heavy-haul railway tunnels in service, it was found that these diseases are mainly concentrated to the bottom of the tunnel structure, for example, the deterioration of and cavity formation in the surrounding rock of the tunnel bottom, sinking of the basement, and mud pumping (Li, 2018; Lazorenko et al., 2019; Singh, 2019; Li et al., 2021). According to the disease situation, the train load is one of the major factors affecting the damage to the bottom of a heavy-haul railway tunnel. Combined with the effect of groundwater, the diseases of a tunnel bottom will further increase and endanger the safety of tunnel operation. Therefore, the evolution law of such diseases must be studied in the case of heavy-haul railway tunnels under the coupling effect of train load and groundwater.

At present, research on the formation and development of diseases of the bottom of heavy-haul railway tunnels under the coupling effect of train load and groundwater has achieved certain results. In the field investigation of heavy-haul railway tunnel diseases, the study by Mandal and Singh (2009) shows that when the tunnel is located in weak surrounding rock, the tunnel structure is strongly squeezed under large geological tectonic stress. Li Ziqiang (Li et al., 2019) determined that the diseases to the tunnel bottom are mainly manifested as basement surrounding rock cavities, especially under the combined action of groundwater and train load. Based on the plastic damage constitutive model of concrete, Ding Zude (Ding et al., 2012) found that the dynamic response and damage to the bottom structure of the tunnel increased with an increase in the cavity distance after the cavity occurred at the bottom of the tunnel. Based on the structural dynamics theory, Fan Xiangxi (Fan et al., 2018) analyzed the dynamic response of the tunnel structure under a train dynamic load and the change in the surrounding rock seepage field. Their results showed that the train dynamic load can significantly improve the water pressure of water-rich tunnels without considering the influence of waterproofing and drainage methods. Jia Chaojun (Jia et al., 2020) derived the damage evolution law of brittle rock surrounding rock under water-force coupling based on an elastic–plastic damage model. Joo and Shin (Joo and Shin, 2013) confirmed the relationship between pore water pressure and inflow rate. Su Haijian (Su, 2015) proposed a numerical method for calculating the degradation effect of surrounding rock under groundwater. Gao Liping (Gao et al., 2020) established a three-dimensional model of train load-tunnel-surrounding rock with an axle load of 300 kN, and divided the different degrees of the tunnel basement cavity into four grades: safety, alertness, danger, and extreme danger. Zhang Dongmei (Zhang et al., 2003) established a viscoelastic rheological model of a soft soil tunnel based on the Terzaghi consolidation theory and obtained tunnel settlement characteristics and settlement stability time. Liu Xinrong (Liu et al., 2012) studied the interaction between water and rock and found that the deterioration of rock was mainly caused by the coupling of seepage and stress. Khamitov et al. (Khamitov et al., 2021) established a contact bond model to determine the damage range and discrete particle trajectory of weakly cemented sandstone during perforation and sand production. Wang Nianyi (Wang et al., 2016a) analyzed and summarized the variation law of water and soil pressure of heavy-haul railway tunnels under train loads and found that the dynamic influence of water and soil pressure of the surrounding rock of the tunnel base was mainly concentrated in the arch bottom and below the track. In summary, the surrounding rock cavity at the bottom of a heavy-haul railway tunnel is mainly caused by defects in the surrounding rock, train load, and groundwater. However, owing to the lack of field measured data, most of the research results are based on qualitative research of theoretical analysis and numerical simulation, and differ considerably from each other.

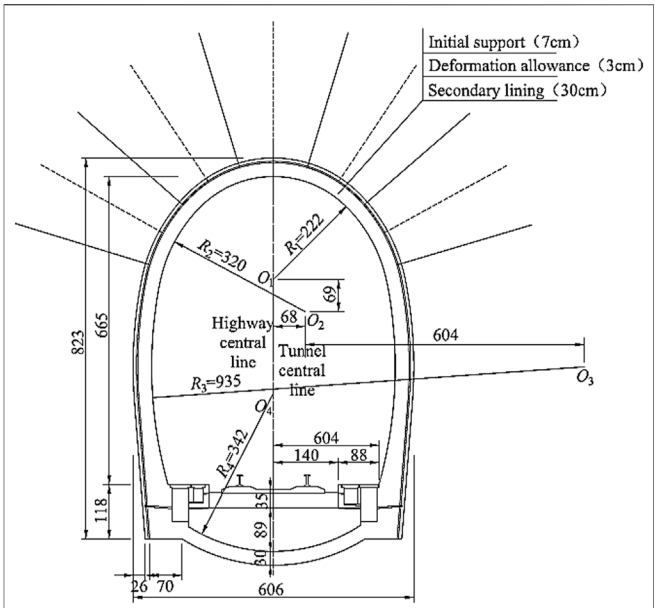

FIGURE 1 | Lining section of Taihangshan Mountain Tunnel (unit: cm).

In this study, based on the engineering of the Taihangshan tunnel of the Wali line, according to the measured data of contact pressure and water pressure on the surface of the surrounding rock at the bottom of the tunnel, the phenomenon of surrounding rock degradation and cavity was explored. Combined with the actual conditions at the site, a laboratory test was conducted to explore the evolution law of the surrounding rock under the coupling effect of train load and groundwater, and the scope and degree of the cavity are quantitatively analyzed.

FIELD LONG-TERM MONITORING

Engineering Situation

This study is based on the Taihang Mountain Tunnel of Wali Railway, which is the first railway built according to the standard

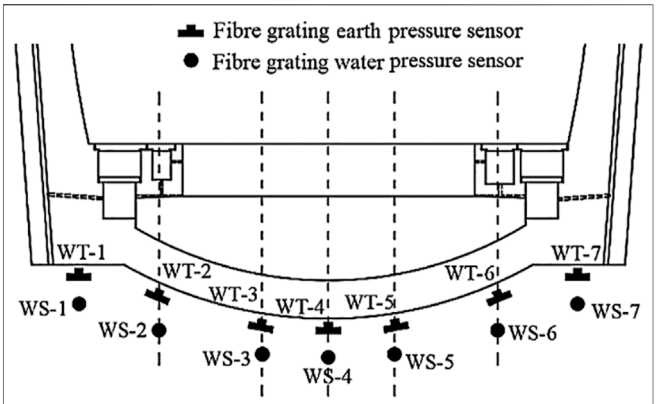

FIGURE 2 | Schematic layout of bottom surrounding rock sensors.

300-kN heavy-haul railway in China. Taihang Mountain is the third double-hole, single-line heavy-haul railway tunnel in China. A ballastless slab track structure is adopted in the tunnel. Curves were set in the inlet and outlet sections, and the remaining sections are straight lines. The length of the left tunnel is 18.125 km (DK 578 + 875–DK 597 + 000), and the right tunnel is 18.108 km (DYK 578 + 865–DYK 596 + 973). The actual axle load of the heavy-haul train in the Taihang Mountain Tunnel is 300 kN, the designed speed is 120 km/h, and the actual opening speed is 80 km/h. The daily traffic includes approximately 16 heavy-haul trains, with annual traffic exceeding 40 million tons. The hydrogeological conditions of the section where the tunnel is located are complex, and groundwater is developed in some mileages. The lining is illustrated in **Figure 1**.

Detection Scheme

Measuring Point Arrangement

To measure the distribution and variation in the water pressure and contact pressure of the surrounding rock of the tunnel basement under the long-term load of the heavy-haul train, the measuring points, as shown in **Figure 2**, were symmetrically arranged on the surface of the bottom surrounding rock, arch foot, bottom of the side ditch, bottom of the track, and center of the line (Goh et al., 2018; Zhang et al., 2020a). The geological condition of the sensor buried section is class V surrounding rock, and the buried depth is 872 m.

In the long-term monitoring process of the Taihang Mountain Tunnel, the measuring range of the soil pressure gauge (WT-1–WT-7) on the surrounding rock surface was 2 MPa, and the measuring range of the water pressure gauge (WS-1–WS-7) was 700 kPa. The sampling frequency was 100 Hz, that is, the sampling time interval was 0.01 s.

Test Sensors

In view of the complex hydrogeological conditions of the Taihang Mountain Tunnel, it is necessary to meet the requirements of strong anti-interference, long-term durability, and stable test data when selecting test sensors. Therefore, the long-term monitoring employed in this study uses fiber grating water and soil pressure sensors.

REMOTE MEASUREMENT RESULTS

Because the tunnel structure is statically indeterminate, it is bound to accumulate stress on the surrounding rock of the tunnel bottom under the action of high-frequency reciprocating trains during operation. This cumulative effect also directly affects the long-term change in the contact and water pressures of the surrounding rock at the bottom.

Long–Term Variation in Contact Pressure of the Bottom Rocks

To systematically study the variation law of the contact pressure of the surrounding rock at the bottom, the long-term variation law of the contact pressure of the rock was divided into four characteristic stages (before operation, 1 month, 6 months, and 1 year) according to the measured data analysis, as shown in **Table 1** and **Figure 3**.

As shown, the surrounding rock at the bottom of the Taihang Mountain tunnel is only disturbed by the construction stage before operating the tunnel. The surrounding rock at the bottom shows that the contact pressure distribution at each measuring point is uniform, with the maximum contact pressure of 51.419 kPa below the left rail. For a single-track railway tunnel, the transverse distribution of the base contact pressure should theoretically be symmetrical. However, because of factors, such as site construction methods and geological conditions, the inverted arch structure and the bottom surrounding rock cannot be fully fitted, resulting in a transverse distribution of the contact pressure.

After 1 month of operation, the contact pressure of each measuring point in the bottom surrounding rock increased, and the maximum contact pressure below the left rail was still 61.445 kPa. This phenomenon indicates damage between the inverted arch structure below the left rail and the bottom surrounding rock and implies a small deviation in the position

TABLE 1 | Contact pressure of surrounding rock of Taihangshan tunnel basement (kPa).

Traffic state	Left arch foot	Bottom of left ditch	Left track	Arch bottom	Right track	Bottom of right ditch	Right arch foot
Before operation	23.524	30.118	51.419	36.410	37.670	48.901	21.651
One month	28.324	38.181	61.445	57.345	53.465	50.657	24.310
Six months	40.563	89.129	84.129	72.997	62.766	73.806	23.245
One year	78.486	142.505	113.944	137.812	93.169	122.846	32.444

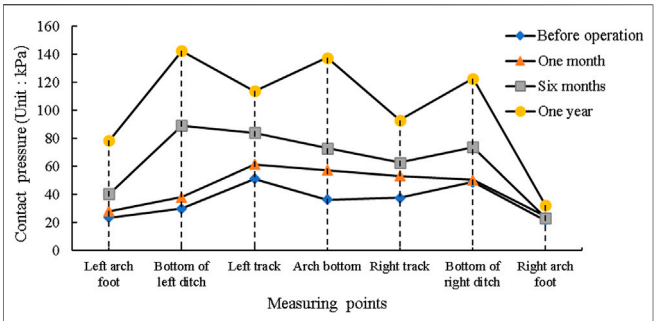

FIGURE 3 | Contact pressure of surrounding rock at the bottom of Taihangshan tunnel (unit: kPa).

of the earth pressure sensor. Under the load of a heavy-haul train, reciprocating rolling aggravates the damage to form a local cavity, resulting in an increase in the contact pressure.

After 6 months of operation, the contact pressure at the bottom of the left ditch on the surrounding rock surface increased to a maximum of 89.129 kPa. The increase in contact pressure at the adjacent positions of the left rail measuring point (the bottom of the left ditch and the arch bottom) was 195.9% and 100.5%, respectively. This phenomenon shows that with the increase in operation time, the damage cavity range of the surrounding rock at the tunnel bottom gradually expands to the adjacent measuring points.

After 1 year of operation, the measuring points at the bottom of the left ditch and arch bottom increased most obviously. The contact pressure at the bottom of the left ditch increased from 30.118 to 142.505 kPa, with an increase of 373.16%. The arch bottom measuring point increased by 278.5% from 36.410 to 137.812 kPa. The long-term effect of the contact pressure on the surface of the bottom surrounding rock is not the same after opening; however, the overall increment of the left is significantly higher than that of the right. According to this development law, it is easy to cause instability in the basement structure and affect the operation safety.

Long-Term Variation of Water Pressure in Bottom Rock

The uneven distribution of contact pressure was caused by groundwater erosion on the surrounding rock under heavy-haul train loads. To clarify the change in water pressure, the long-term change in hydrodynamic pressure was divided into four stages (before operation, 1 month, 6 months, and 1 year) and analyzed. The hydrodynamic pressures are listed in **Table 2**; **Figure 4**.

As shown, the maximum hydrodynamic pressure of the Taihangshan tunnel before operation is 111.765 kPa, which is located below the left track. The main reason for the large water pressure at this measuring point is that during the construction stage, the empty slag of the base surrounding rock is not completely cleared during the inverted arch pouring, resulting in a large gap between the surrounding rock and inverted arch structure, and thus allowing space for groundwater to seep in and cause high hydrodynamic pressure owing to the disturbance of the construction on the surrounding rock.

After 1 month of operation, the water pressure at each measuring point increased. The local cavity beneath the left rail and the combined action of heavy-haul train load and groundwater make the water pressure at this position the maximum, which is 184.804 kPa. The maximum increase in the water pressure at the arch bottom is 143.2%.

After half a year of operation, under the long-term action of heavy-haul train load and groundwater, the surrounding rock damage under the track was intensified, and the cavity was developed. The maximum water pressure at this location on the lateral distribution was 239.804 kPa.

After 1 year of operation, the water pressure at the left rail measuring point increased from 111.765 to 250.931 kPa. With an increase in the cavity range, the hydrodynamic pressure of the adjacent measuring points, namely, the bottom of the left ditch and the arch bottom, also increased continuously. The largest increase was the increase in the arch bottom measuring point by 243.4%.

According to the analysis of the variation in water pressure at each measuring point, the dynamic water pressure increases with the increase in the degree of cavity, indicating that the load of the heavy-haul train intensifies the erosion of groundwater on the surrounding rock, expanding the surrounding rock gap, and intensifying the accumulation of groundwater. In view of the flow of water to places with low terrain, this phenomenon is the most obvious at the bottom of the surrounding rock arch for the single-track railway tunnel.

LABORATORY TEST DESIGN OF BOTTOM SURROUNDING ROCK CAVITY

According to the analysis results of the contact pressure and water pressure of the surrounding rock at the base of the Taihang Mountain Tunnel, after the heavy-haul railway tunnel

TABLE 2 | Water pressure of surrounding rock of Taihangshan tunnel basement (kPa).

Traffic state	Left arch foot	Bottom of left ditch	Left track	Arch bottom	Right track	Bottom of right ditch	Right arch foot
Before operation	50.673	58.605	111.765	38.528	54.694	36.000	18.605
One month	87.420	88.257	184.804	93.714	99.587	56.530	30.620
Six months	112.358	87.623	239.804	100.173	104.070	63.289	33.470
One year	133.453	139.389	250.931	132.294	122.523	84.622	38.625

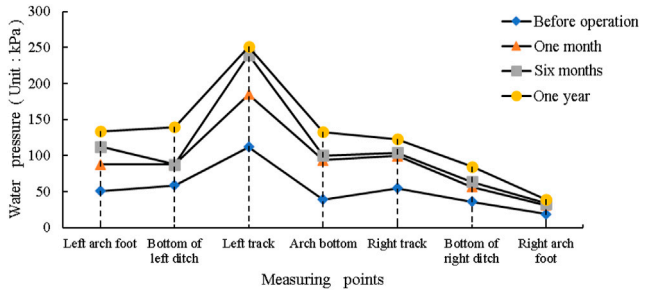

FIGURE 4 | Water pressure of surrounding rock at the bottom of Taihangshan tunnel (unit: kPa).

TABLE 3 | Dynamic similarity constants of laboratory tests.

Physical quantity	Similitude parameter
Geometrical dimension L /m	$C_L = 20$
Pressure P /kPa	$C_P = 20$
Quality density Cρ/Kg · m^{-3}	$C\rho = 1$
Elastic modulus C_{Ed} /Pa	$C_{Ed} = 20$
Poisson ratio μd	$C_{\mu d} = 1$
Vibration (loading) frequency ω(l/s)	$C_\omega = C_L^{1/2} = 4.47$
Gravity g /m·s^{-2}	$Cg = 1$
Duration of input vibration T /s	$C_T = C_L^{-1/2} = 0.224$
Dynamic response stress σd/Pa	$C_{\sigma d} = C_L = 20$
Dynamic response line displacement Sd /m	$C_{Sd} = C_L = 20$
Dynamic response deformation ε_d	$C\varepsilon_d = 1$
Physical quantity	Similitude parameter
Dynamic response acceleration a /m·s^{-2}	$C_a = 1$
Dynamic response pore water pressure u /Pa	$C_u = C_L = 20$

TABLE 4 | Dynamic similarity constants of model tests.

Test parameters	Dynamic similarity constant
Permeability coefficient k /m·s^{-1}	$C_k = 1$
Flow velocity v /m·s^{-1}	$C_v = C_k = 1$
Water head height H /m	$C_H = C_L = 20$
Seepage quantity Q/m^3·s^{-1}	$C_Q = C_L^2\, C_k = 400$

was put into use, with an increase in operation time, the bottom surrounding rock was damaged and deteriorated under the influence of groundwater and large axle load; this affected the operational safety of the tunnel structure. It was predicted that the deterioration of the bottom surrounding rock was due to the erosion of the surrounding rock by groundwater and the loss of surrounding rock particles, resulting in cavities and cracks.

Based on the measured water–soil pressure, a laboratory test was established to simulate the cavity characteristics and formation mechanism of three types of surrounding rock: pebble soil, clay soil, and sandy soil. Among them, the cavity mechanism of the bottom structure of the heavy-haul railway tunnel was qualitatively obtained by studying the defect location, defect degree, soil pressure value of the bottom surrounding rock, and the degree of soil particle loss.

Principle of Experimental Design

Based on the similarity theorem, the geometric similarity ratio between the test model and prototype was 1:20, the similarity ratio of mass density was 1:1, and the similarity ratio of the elastic modulus of the surrounding rock and concrete inverted arch plate was 1:20. The bottom structure of Taihang Mountain adopts plain concrete; that is, the reinforcement is not conducted using the bottom structure model. The similarity constants of other physical quantities derived from the π theorem are listed in **Table 3**.

According to the seepage mechanics of the rock mass, the water movement along the rock gap obeys Darcy's law. The similarity constants of the fluids can be obtained by dimensional analysis, as shown in **Table 4**.

Test Materials and Simulation Devices

Test Material Parameters

The similar materials of the surrounding rock in this laboratory test were simulated by class V surrounding rock. Based on the physical and mechanical parameters of the Code for the design of railway tunnels (Ministry of Railways (200, 2005) class V, surrounding rock, and the actual situation of the Taihangshan tunnel surrounding rock, the range of physical and mechanical parameters of similar materials in the laboratory test of the surrounding rock was determined, as shown in **Table 5**.

To study the cavity characteristics and degree of degradation of various types of surrounding rocks, three representative soil surrounding rocks, namely, pebble soil, clay soil, and sandy soil, with high observability in a relatively short period of time, were selected for the study in a laboratory.

The tunnel bottom structure adopts a simplified model, and the inverted arch filling and inverted arch structure were regarded as the overall structure and prefabricated with gypsum. The inverted arch of the Taihang Mountain Tunnel was filled with C20 concrete, and C30 concrete was used as the inverted arch structure. Therefore, the concrete label of the tunnel bottom structure in this laboratory test was regarded as C25 for the simulation. According to the literature (*Similarity Theory and Structural Model Test*) (Yang, 2005; Wu et al., 2013; Wang et al.,

TABLE 5 | Physical and mechanical parameters of Class V surrounding rock prototype and similar materials.

Class V	Unit weight γ (kN/m^3)	Deformation modulus *E* (MPa)	Poisson ratio υ	Internal friction angle φ (°)	Cohesion *C* (kPa)
Prototype materials	17–20	1,000–2000	0.35–0.45	20–27	50–200
Similar materials	17–20	50–100	0.35–0.45	20–27	2.5–10

TABLE 6 | Comparison of concrete materials of tunnel basement structure.

Mechanical parameter	Prototype value (C25)	Model values
Uniaxial compressive strength	17	0.85
Elastic modulus	29.5	1.475

2016b; Zheng et al., 2017) and previous production experience, the mixture ratio of water, gypsum, and diatomite was determined as 1:0.8:0.2. The mechanical parameters of the concrete prototype and model are listed in **Table 6**.

Training the Simulation Device

The vibration motor 100 W belt governor was selected for the simulation, and the maximum excitation force could reach 130 kg. According to the dynamic load of a 300-kN heavy-haul train obtained by the excitation test, combined with the dynamic similarity ratio of the laboratory test, the excitation force was increased by 10 times as that applied to the surface of the tunnel bottom structure at 100 kPa.

Model Equipment

The self-designed test box was used for testing, and the test box was made of an organic glass plate to facilitate changes in the surrounding rock model and real-time measurement records (Zhang et al., 2020b). A consolidated flume was set on both sides of the main test box, and the water conveyance channel was set on the side wall of the flume to form a connecting device in the main test box, which provides water supply between the tunnel bottom structural model and the bottom surrounding rock. The size of the main test box was 30 cm × 30 cm × 40 cm, and the size of the two sides of the flume was 10 cm × 10 cm × 40 cm. The material similar to the tunnel bottom structure and a device with simulation of train were set inside the test box, as shown in **Figure 5**.

As shown in **Figure 5**, 1–8 structures are as follows: 1, main test box; 2, left flume; 3, right flume; 4, train load simulation device (exciter); 5, material similar to bottom surrounding rock; 6, material similar to tunnel bottom structure; 7, test water storage; and 8, test bench; 9, water conveyance pipeline. The test bench was used to offset the dynamic effect of the exciter, as a detachable structure, and it cannot be set.

Test Conditions

This laboratory simulation test was mainly conducted to study the cavity characteristics and formation mechanism of three types of surrounding rocks under the combined action of heavy-haul train load and groundwater. The simulation opening time was 1 year, and the test time was approximately 118 h. The test conditions are listed in **Table 7**.

LABORATORY TEST RESULTS

In this laboratory test, the characteristics and formation mechanism of the cavity and degradation of the surrounding rock at the tunnel bottom under the combined action of heavy-haul train and groundwater were simulated for three types of surrounding rocks: pebble soil, clay soil, and sandy soil. Heavy-haul train load will further promote the erosion of groundwater on the surrounding rock, and under the same conditions of cavity, different types of surrounding rocks form and their distribution range is different.

Surrounding Rock of Pebble Soil

The laboratory test results of the pebble soil surrounding the rock under water-rich conditions are shown in **Figure 6**.

As shown in **Figure 6**, before the water-rich excitation test, the surface of the surrounding rock of the pebble soil was uniform, and there was no obvious bump phenomenon. After water-rich excitation, the grooves in the middle line were visible, and pebbles sank further owing to their weight. The mud sand was affected by the excitation force and the outlet of the flume, which gathered at the top of the surrounding rock and flowed into the groove to form a catchment area. Under the action of excitation, the light mud sand in the surrounding rock of pebble soil flowed out from the outlet of the flume, and approximately 941 g of fine particles was lost after excitation.

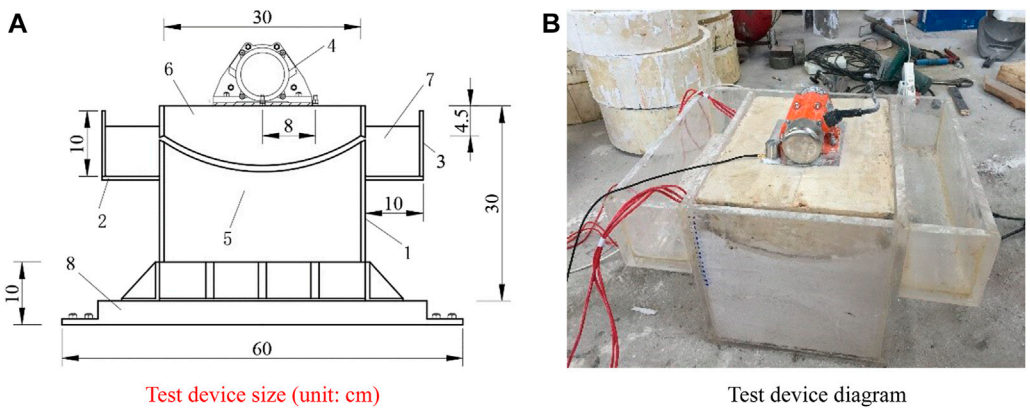

FIGURE 5 | Evacuation test device for tunnel basement structure. **(A)** Test device size (unit: cm). **(B)** Test device diagram.

TABLE 7 | Test conditions.

Serial number	Tunnel bottom structure type	Rock condition	Hydrographic condition	Excitation times /10,000 times
1	Invert structure	Pebble soil	Water-rich	2.53×10^3
2		Clay soil		
3		Sandy soil		

FIGURE 6 | Excitation of water-rich surrounding rock of pebble soil.

FIGURE 7 | Excitation of water-rich surrounding rock of clay soil.

Clay Soil Surrounding Rock

The laboratory test results of the clay surrounding rock under water-rich conditions are shown in **Figure 7**.

As observed, the surrounding rock morphology of clay soil before water-rich excitation is basically consistent with that of the anhydrous condition, and the clay property between particles of clay soil surrounding rock under water-rich conditions is enhanced, and the whole cohesive soil is stable and homogeneous. After water-rich excitation, owing to the lack of large-sized aggregates in the clay surrounding rock, the surrounding rock gradually changes from plasticity to flow plasticity under excitation. Because the plasticity of the surrounding rock weakens the active pore water between the surrounding rock particles and carries more clay particles, the cavity phenomenon is most obvious at the opening of the flume on the side of the test box owing to the high flow velocity. After excitation under water-rich conditions, the clay particles lost approximately 1,415 g.

Sandy Surrounding Rock

The laboratory test results of the sandy soil surrounding rock under water-rich conditions are shown in **Figure 8**.

As observed, the integrity of the sandy soil surrounding rock before water-rich excitation is good, and the distribution of surrounding rock particles on the surface of the bottom surrounding rock is relatively uniform without obvious defects. After water-rich excitation, the soil particles on the surface of the sandy soil surrounding the rock are no longer evenly distributed and appear uneven. Under the action of dynamic load, groundwater scours the bottom surrounding rock, and soil particles enter the flume on both sides through the water channels, thus forming a number of water channels on the surface of the sandy soil surrounding rock, thereby accelerating the formation of the cavity surrounding the rock.

There are three hard soil blocks with obvious uplift at the interface between the inverted arch structure and sandy soil surrounding the rock, and they are distributed along the corresponding positions of the two sides of the track. The main reason for the formation of the soil block is that under the combined action of heavy-haul train load and groundwater, the compactness of the sandy soil surrounding the rock is different in different regions after water erosion. The loose soil particles are eroded by water erosion, and an area with a large consolidation strength is gradually formed. After water-rich

FIGURE 8 | Excitation of water-rich surrounding rock of sandy soil.

excitation, the weight loss of the sandy soil particles is approximately 858 g.

Comprehensive Analysis of Laboratory Test Results

Under the condition of rich water, after the long-term action of heavy-haul train simulation load, the tunnel bottom structure of sandy soil surrounding the rock is characterized by large hanging area. The cavity characteristics of the tunnel bottom structure in the clay surrounding the rock are characterized by a large hanging area with a partial uplift soil block. The cavity characteristics of the tunnel bottom structure of the pebble soil surrounding rock are shown as local cavities. It can be seen that the cavity characteristics of the tunnel bottom structure are mainly determined by the surrounding rock properties.

Under water-rich conditions, the cavity characteristics of different surrounding rocks are different after the heavy-haul train simulates the long-term load, and different degrees of particle loss occur. Among them, the loss of clay surrounding the rock is the most significant, reaching 1,415 g, which is 50.3% higher than that of the pebble soil surrounding rock and 64.9% higher than that of the sandy soil surrounding rock, which directly affects the range and depth of cavity deterioration of the bottom surrounding rock.

CONCLUSION

Based on the measured data of water and soil pressure in the Taihang Mountain tunnel, this study investigated the mechanism of the structural cavity at the bottom of the tunnel, and discussed the cavity characteristics and degradation depth of pebble soil, clay soil, and sandy soil under the combined action of heavy-haul trains and groundwater. The following conclusions can be drawn.

1) For a heavy-haul railway tunnel under water-rich conditions, the objective defects of the bottom surrounding rock after the completion of construction continue to develop and deteriorate under the combined action of groundwater and train load. Thus, the soil and water pressures of the bottom surrounding rock continue to increase with the increase in the operation time, resulting in the instability of the tunnel base and affecting the operation safety.
2) Laboratory tests showed that the cavity characteristics of different surrounding rocks differ from each other. The cavity characteristics of the pebble soil surrounding rock are mainly characterized by small-scale local cavities, while that of the clay soil surrounding rock are overall hanging, and sandy soil surrounding rock are convex with local soil blocks.
3) Under the same test conditions, among the three typical types of surrounding rock, the clay soil surrounding rock had the largest particle loss of 1,310 g, which was 64.9% higher than that of 941 g of the pebble soil surrounding rock and 50.3% higher than that of 858 g of the sandy soil surrounding rock. Special attention should be paid to the deterioration and damage of the bottom surrounding rock in the weak surrounding rock area with rich water environment.
4) In the design and construction process of heavy-haul railway tunnels, especially in the condition of rich water, in addition to the safety of the bottom structure under a train impact load, it is also necessary to compare and select the design scheme of the bottom structure according to geological and groundwater conditions. In the construction process, more attention should be paid to the treatment of the bottom slag to improve the construction quality.

DATA AVAILABILITY STATEMENT

The original contributions presented in the study are included in the article/Supplementary Material, further inquiries can be directed to the corresponding author.

AUTHOR CONTRIBUTIONS

ZL: Overall thinking and thesis writing. KC: Data analysis, paper modification, and coloring. ZL: Experimental design. WH: Literature research and data analysis. XW: Data collation.

FUNDING

The constructive comments and suggestions made by the Open-end Fund of Key Laboratory of New Technology for Construction of Cities in Mountain Area (LNTCCMA-20210108), the

Chongqing Talent Plan (CQYC2020058263), Chongqing Natural Science Fund General Project (cstc2020jcyj-msxmX0904), Chongqing Talents : Exceptional Young Talents Project (cstc2021ycjh-bgzxm0246), China Postdoctoral Science Foundation- General Project (2021M693739), the National Natural Science Foundation of China (5108098).

REFERENCES

Ding, Z., Peng, L., Huang, J., and Shi, C. (2012). Traffic Safety Analysis of Railway Tunnel under the Condition of Base Void. *J. railways* (09), 104–110. doi:10.3969/j.issn.1001-8360.2012.09.018

Fan, X., Yang, J., Ma, Y., Miao, D., and Ma, T. (2018). Dynamic Analysis of Fushui Tunnel under Train Vibration Load under Different waterproof and Drainage Methods. *J. Railway Sci. Eng.* 15 (11), 187–194. doi:10.19713/j.cnki.43-1423/u.2018.11.022

Khamitov, F., Minh, N. H., and Yong, Z. (2021). Coupled CFD–DEM Numerical Modelling of Perforation Damage and Sand Production in Weak sandstone Formation. *Geo. Engy. Env.* 28, 100255. doi:10.1016/j.gete.2021.100255

Gao, L., Luo, J., and Wang, L. (2020). Analysis on Vibration Characteristics and Life Prediction of Inverted Arch under the Condition of Base Void. *J. civil Eng.* 53 (S1), 348–354. doi:10.15951/j.tmgcxb.2020.s1.055

Goh, A. T. C., Zhang, W., Zhang, Y., Xiao, Y., and Xiang, Y. (2018). Determination of Earth Pressure Balance Tunnel-Related Maximum Surface Settlement: a Multivariate Adaptive Regression Splines Approach. *Bull. Eng. Geol. Environ.* 77, 489–500. doi:10.1007/s10064-016-0937-8

Hong, L. (2000). An Overview of Foreign Heavy Haul Railway. *Railway Eng. J.* (4), 32–34. doi:10.3969/j.issn.1006-2106.2000.04.009

Jia, C., Wang, Y., Gong, C., Lei, M., and Shi, C. (2020). Study on Constitutive Model of Tunnel Surrounding Rock under Water Force Coupling. *J. underground Space Eng.* 16 (126(S1)), 106–113.

Joo, E. J., and Shin, J. H. (2013). Relationship between Water Pressure and Inflow Rate in Underwater Tunnels and Buried Pipes. *Géotechnique* 64 (3), 226–231. doi:10.1680/geot.12.p.185

Lazorenko, G., Kasprzhitskii, A., Khakiev, Z., and Yavna, V. (2019). Dynamic Behavior and Stability of Soil Foundation in Heavy Haul Railway Tracks: A Review. *Construction building Mater.* 205, 111–136. doi:10.1016/j.conbuildmat.2019.01.184

Li, Z., Huang, W., Xu, Z., Tang, X., Wang, M., Yu, L., et al. (2021). Analysis of the Mechanical Characteristics of Different Track Bed Types in Heavy-Haul Railway Tunnels. *Math. Probl. Eng.* 2021 (2), 1–11. doi:10.1155/2021/5527073

Li, Z. (2018). *Dynamic Characteristics and Design Method of Heavy Haul Railway Tunnel Structure*. Chengdu: Southwest Jiaotong University.

Li, Z., Wang, N., Yu, Li., and Xu, Z. (2019). Study on Damage Mechanism of Surrounding Rock at the Bottom of Heavy Haul Railway Tunnel. *J. railways* 41 (07), 162–170. doi:10.3969/j.issn.1001-8360.2019.07.021

Liu, X., Fu, Y., Zheng, Y., and Liang, N. (2012). Study on the Influence of Water Rock Interaction on Rock Degradation. *J. underground Space Eng.* (01), 77–82. doi:10.3969/j.issn.1673-0836.2012.01.013

Mandal, S. K., and Singh, M. M. (2009). Evaluating Extent and Causes of Overbreak in Tunnels. *Tunnelling Underground Space Tech.* 24 (1), 22–36. doi:10.1016/j.tust.2008.01.007

Ministry of Railways (2005). *TB10003-2005 Code for Design on Tunnel of Railway*. Beijing: China Railway Publishing House.

Singh, M. (2019). Subgrade Instability and Fluidisation under Cyclic Railway Loading. Philosophy thesis. Wollongong(Australia): University of Wollongong.

Su, H. (2015). *Seepage Evolution Mechanism and Engineering Application of Deep Jointed Rock Mass*. Xuzhou: China University of mining and technology.

Wang, K., Li, S., Zhang, Q., Zhang, X., Li, L., Zhang, Q., et al. (2016). Development and Application of New Similar Materials for Fluid - Solid Coupling Model Test. *Geotechnics* 37 (09), 2521–2533.

Wang, N., Luo, Y., Li, Z., et al. (2016). Dynamic Study on Water and Soil Pressure of Surrounding Rock at the Base of Heavy Haul Railway Tunnel. *Hydrogeology Engineering Geology.* 43 (4), 96–102. doi:10.16030/j.cnki.issn.1000-3665.2016.04.16

Wu, B., Zhu, H., Xu, Q., and Ming, J. (2013). Experimental Study on Similar Materials of Grade IV Weak Surrounding Rock. *Geotechnics* 34 (S1), 109–116.

Wu, Q., Li, Z., Yu, Li., Huayang, Y., and Wang, M. (2017). Experimental Study on Long-Term Dynamic Characteristics of Base Structure of Heavy Haul Railway Tunnel. *Vibration and impact* 36 (10), 127–133. 167. doi:10.13465/j.cnki.jvs.2017.10.021

Yang, J. (2005). *Similarity Theory and Structural Model Test*. Wuchang: Wuhan University of Technology Press.

Zhang, D., Huang, H., and Wang, J. (2003). Coupling Analysis of Viscoelastic Rheology and Consolidation of Long-Term Ground Settlement of Soft Soil Tunnel. *J. rock Mech. Eng.* 22 (0z1), 2359–2362. doi:10.3321/j.issn:1000-6915.2003.z1.049

Zhang, W., Zhong, H., Zeng, Z. K., Wu, D. F., and Zhang, Y. (2020). Visualization and Digitization of Model Tunnel Deformation via Transparent Soil Testing Technique. *Underground Space* 2020 (1). doi:10.1016/j.undsp.2020.05.004

Zhang, W. G., Li, H. R., Wu, C. Z., Li, Y. Q., Liu, Z. Q., and Liu, H. L. (2020). Soft Computing Approach for Prediction of Surface Settlement Induced by Earth Pressure Balance Shield Tunneling. *Underground Space* 6, 353–363. doi:10.1016/j.undsp.2019.12.003

Zheng, L., He, C., Gao, X., Yang, S., Luo, Y., and Yang, W. (2017). Development and Application of Similar Materials for Rock Tunnel Seepage Model Test. *J. Harbin Inst. Tech.* 49 (09), 33–39. doi:10.11918/j.issn.0367-6234.201607075

Zou, W., Zhang, M., Liu, Y., and Ma, W. (2016). 30t Axle Load of Heavy Haul Railway Tunnel Basement Structure Stress Distribution and Dynamic Response. *China Railway Sci.* 37 (05), 50–57. doi:10.3969/j.issn.1001-4632.2016.05.07

Conflict of Interest: The handling editor declared a shared affiliation with with the authors (ZL, KC, ZL, WH, XW) at time of review.

Author ZL was employed by the company Chongqing City Construction Investment (Group) Co., Ltd.

The remaining authors declare that the research was conducted in the absence of any commercial or financial relationships that could be construed as a potential conflict of interest.